Accepted Manuscript

Design and synthesis of tranylcypromine derivatives as novel LSD1/HDACs dual inhibitors for cancer treatment

Ying-Chao Duan, Yong-Cheng Ma, Wen-Ping Qin, Li-Na Ding, Yi-Chao Zheng, Ying-Li Zhu, Xiao-Yu Zhai, Jing Yang, Chao-Ya Ma, Yuan-Yuan Guan

PII: S0223-5234(17)30752-3

DOI: 10.1016/j.ejmech.2017.09.038

Reference: EJMECH 9753

To appear in: *European Journal of Medicinal Chemistry*

Received Date: 1 July 2017

Revised Date: 18 September 2017

Accepted Date: 19 September 2017

Please cite this article as: Y.-C. Duan, Y.-C. Ma, W.-P. Qin, L.-N. Ding, Y.-C. Zheng, Y.-L. Zhu, X.-Y. Zhai, J. Yang, C.-Y. Ma, Y.-Y. Guan, Design and synthesis of tranylcypromine derivatives as novel LSD1/HDACs dual inhibitors for cancer treatment, *European Journal of Medicinal Chemistry* (2017), doi: 10.1016/j.ejmech.2017.09.038.

Compound 7: LSD1/HDACs dual inhibitor

LSD1 IC_{50} : 1.20 μM
HDAC1 IC_{50} : 15 nM
HDAC2 IC_{50} : 23 nM
Potent anticancer activity IC_{50} : 0.81~5.48 μM

Design and synthesis of tranylcypromine derivatives as novel LSD1/HDACs dual inhibitors for cancer treatment

Ying-Chao Duan[a*], Yong-Cheng Ma[b], Wen-Ping Qin[a], Li-Na Ding[c], Yi-Chao Zheng[c] Ying-Li Zhu[b], Xiao-Yu Zhai[a], Jing Yang[c], Chao-Ya Ma[c], Yuan-Yuan Guan[a**]

[a] *School of Pharmacy, Xinxiang Medical University, Xinxiang, Henan 453003, China.*
[b]*Department of Pharmacy, Zhengzhou University People's Hospital, No. 7, Wei Wu Road, Zhengzhou, Henan,China*
[c]*Key Laboratory of Advanced Drug Preparation Technologies(Zhengzhou University) , Ministry of Education; Collaborative Innovation Center of New Drug Research and Safety Evaluation, Henan Province; Key Laboratory of Henan Province for Drug Quality and Evaluation; School of Pharmaceutical Sciences, Zhengzhou University, 100 Kexue Avenue, Zhengzhou, Henan 450001, China.*

* Corresponding authors
E-mail address:duanyingchao1986@163.com (Y.C. Duan)
E-mail address:131011@xxmu.edu.cn (Y.Y. Guan)

Abstract

Lysine specific demethylase 1 (LSD1) and Histone deacetylases (HDACs) are promising drug targets for cancers. Recent studies reveal an important functional interplay between LSD1 and HDACs, and there is evidence for the synergistic effect of combined LSD1 and HDAC inhibitors on cancers. Therefore, development of inhibitors targeting both LSD1 and HDACs might be a promising strategy for epigenetic therapy of cancers. We report herein the synthesis of a series of tranylcypromine derivatives as LSD1/HDACs dual inhibitors. Most compounds showed potent LSD1 and HDACs inhibitory activity, especially compound **7** displayed the most potent inhibitory activity against HDAC1 and HDAC2 with IC_{50} of 15 nM and 23 nM, as well as potent inhibition against LSD1 with IC_{50} of 1.20 μM. Compound **7** demonstrated stronger anti-proliferative activities than SAHA with IC_{50} values ranging from 0.81 to 4.28 μM against MGC-803, MCF-7, SW-620 and A-549 human cancer cell lines. Further mechanistic studies showed that compound **7** treatment in MGC-803 cells dose-dependently increased cellular H3K4 and H3K9 methylation, as well as H3 acetylation, decreased the mitochondrial membrane potential and induced remarkable apoptosis. Docking studies showed that compound **7** can be well docked into the active binding sites of LSD1 and HDAC2. This finding highlights the potential for the development of LSD1/HDACs dual inhibitors as novel anticancer drugs.

Key words: Lysine-specific demethylase 1; Histone deacetylases; dual inhibitor; synthesis

1. Introduction

Diverse epigenetic abnormalities have been directly implicated in the origin, development and metastasis of cancers [1]. Over the past decade, epigenetic therapies for cancer treatment have attracted extensive attention of researchers and clinicians as they provide alternative therapeutic options [2-4]. Epigenetic regulators like lysine specific demethylase1(LSD1) and histone deacetylases (HDACs) are being increasingly used as targets for chemotherapeutic intervention in cancers [5].

LSD1 was the first identified histone demethylase in 2004 [6]. As a component of the CoREST corepressor complex, LSD1 specifically catalyses the demethylation of mono- and di-methylated histone H3 lysine 4 (H3K4) and represses gene transcription [7]. While in the presence of the androgen receptor, it specifically removes mono- or di-methylated H3 lysine 9 (H3K9) and activates gene transcription [8]. LSD1 also demethylates non-histone protein, such as p53 [9], DNA methyltransferases [10], E2F transcription factor 1 (E2F1) [11]and regulates their cellular functions. High level expression of LSD1 was frequently found in malignancies [12]and is associated with development, progression and poor clinical outcome in cancers of the lung [13], acute myeloid leukemia [14, 15], gallbladder [16], colon [17] and breast cancers [18]. Downregulation or inhibition of LSD1 was shown to re-express the epigenetically silenced tumor suppressor genes and inhibit cancer cell proliferation and metastasis [19, 20]. Therefore, LSD1 is regarded as a promising drug target for cancer intervention [21, 22]. A number of LSD1 inhibitors (LSD1i) with various scaffolds, including cyclopropylamine (**1**, **2**), amidoxime(**3**) [23], pyridine(**4**) [24], benzohydrazide(**5**) [25], thieno[3,2-*b*]pyrrole(**6**) [26]and others have been developed [27-30](**Fig. 1**). We have also contributed to the field with the identification of two novel types of LSD1i [31-33]. The most widely studied and potent LSD1i are cyclopropylamine containing compounds, derived from tranylcypromine (2-PCPA) [34, 35], and two of these compounds ORY-1001 (**1**) and GSK2879552(**2**), are in clinical development for the treatment of acute myeloid leukemia [35-37].

HDACs are enzymes responsible for removing the acetyl group from acetylated lysine residues located on histone as well as nonhistone proteins [38, 39]. Such posttranslational modifications are crucial for the regulation of gene expression and cellular processes, including apoptosis, cell cycle, growth and differentiation [40]. The HDAC family consists of 18 proteins, which can be grouped into four different classes based on their sequence homology: class I (HDACs 1-3 and 8), class II (HDACs 4, 5, 6, 7, 9, 10), and class IV (HDAC 11) are all zinc-dependent deacetylases, and class III called Sirtuins (Sirtuins1-7) are the NAD^+-dependent HDACs [41]. Abnormal expression of HDACs has been implicated in the initiation and progression of diverse cancers [42, 43]. Histone deacetylase inhibition has proven to be a valuable epigenetic strategy for cancer treatment [44]. Five HDACs inhibitors (HDACi) (SAHA [45], romidepsine [46], belinostat [47], panobinostat [48] and chidamide [49]) have been approved by FDA (**Fig. 2**), and several other HDACi are currently in different phases of clinical development [50, 51]. HDACi have also been combined with other cancer therapeutics including those targeting DNMT[52], Bcl-2 [53], EGFR [54]or conventional chemotherapeutic agents, such as paclitaxel, gemcitabine, fluorouracil and platinum compounds to treat cancers[55], and showed more effective anticancer activities, many different combination strategies are at various stages of clinical trials against various cancers[56, 57].

Recent studies have revealed that there are intimate functional link between the LSD1 and HDACs. LSD1 and HDACs are found in the same cellular complexes, for example, HDAC1, HDAC2 and LSD1 are the integral subunits of CoREST and NuRD corepressor complexes [7, 58]. HDAC1 deacetylates LSD1 at K374 in the substrate binding lobe, which affects the histone 3 binding and gene expression activity of LSD1 [59]. Overexpression of HDAC5 stabilizes LSD1 protein and decreases the level of H3K4 methylation, whereas loss of HDAC5 diminishes LSD1 protein stability and demethylation activity [60]. HDACi increases H3K4 methylation via transcriptional repression of histone demethylases [61, 62], while inhibition of

LSD1 activity leads to enhanced histone acetylation and sensitizes cancer cells to HDACi-induced apoptosis [63]. HDACi and LSD1i have been tested as combination anticancer agents and showed synergistic effect in human breast cancer [64, 65], AML [66] and glioblastoma multiforme [63, 67].

Both LSD1 and HDACs are overexpressed in many human cancers, resulting in aberrant silencing of tumor suppressor genes, inhibition of their activity can prevent cancer growth, migration and invasion. More importantly, simultaneous inhibition of LSD1 and HDACs exhibits synergistic anticancer activity. Therefore, there is a great interest in developing inhibitors targeting both LSD1 and HDACs for epigenetic therapy of cancers. Herein, a series of tranylcypromine derivatives with pharmacophore characteristics of HDACi were synthesized and evaluated as LSD1/HDACs dual inhibitors.

2. Results and discussion

2.1. Chemistry

Compounds **1-7** and **8-11** were synthesized using the routes described in Schemes 1-2. A commercially available trans-2-phenylcyclopropylamine hydrochloride was reacted with $(Boc)_2O$ in dry dichloromethane to give compound **1**. Compound **1** was treated with methyl 4-(bromomethyl)benzoate or methyl 3-(4-bromomethyl)cinnamate in dry DMF, in the presence of NaH, to give the **2** and **8**, which were then hydrolyzed with Lithium hydroxide to afford compounds **3** and **9**, respectively. Condensation of **3** or **9** with the corresponding amino-compounds in dry DMF at room temperature in the presence of HBTU provided compounds **4** and **10**, respectively. The target compounds **5a-b** and **11a-b** were finally obtained by de-protection of **4a-b** and **10a-b** with trifluoroacetic acid in dichloromethane. For the synthesis of hydroxamate compound **7**, compound **4c** was treated with hydroxylamine in the presence of KOH to produce **6**, which was de-protected with TFA to generate compound **7**.

2.2. In vitro LSD1, MAO-A and MAO-B inhibition

All the synthesized target compounds and SAHA were tested for their inhibitory activity against LSD1 *in vitro*. The data are summarized in **Table 1**. 2-PCPA was chosen as positive control. As shown in **Table 1**, all of the compounds with the exception of exhibited moderate to potent inhibitory activities against LSD1 with IC_{50} values ranging from 1.20 to 7.16 μM, more potent than 2-PCPA, while SAHA showed no inhibition against LSD1. Among them, compounds **7** (IC_{50} = 1.20 μM) showed the most potent anti-LSD1 activities, which are 25 times higher than that of 2-PCPA. As LSD1 belongs to the FAD-dependent monoamine oxidases family including MAO-A and MAO-B, we also analyzed the inhibitory effects of synthesized compounds against MAO-A and MAO-B to assess their selectivity, clorgyline and R-(-)-deprenyl were chosen as positive control for MAO-A and MAO-B, respectively. All the compounds displayed weak MAO-A inhibitory activities, while had no significant effects on MAO-B activities. The results showed that these compounds exhibited better selectivity for LSD1 over MAO A and MAO B, compared to 2-PCPA.

2.3. In vitro HDAC inhibition

To explore the characteristics of target compounds on HDAC inhibition, the inhibitory effects against selected recombinant HDACs-HDAC1, HDAC2 and

HDAC5, which are typically found in association with LSD1, were determined by a fluorescence-based assay. SAHA and TMP269 were used as positive controls. The data are showed as IC_{50} values in **Table 2** below. All target compounds showed good to excellent inhibitory activities against HDAC1 and HDAC2, while had no effect on HDAC5 except for compound **7** and **11a**, which were found to be moderately active with IC_{50} values in micromolar range. Compounds **7** and **11a** displayed the most potent HDAC1/2 inhibitory activity with IC_{50} values 12, 15, 25, and 23 nM, respectively, similar to that of SAHA.

2.4. In vitro anti-proliferative activity

All synthesized target compounds together with the reference compound SAHA were explored for their anti-proliferative activity in five different cancer cell lines, human gastric cancer cells (MGC-803), human breast cancer cell (MCF-7), human colorectal cancer cell (SW-620), human prostate cancer cell (PC-3) and human lung cancer cell (A-549). The results are summarized in **Table 3**. All synthesized compounds manifested evident antiproliferative activities against five cancer cell lines. Compounds **7** and **11a** displayed potent broad-spectrum growth inhibitory activities against all the tested cell lines with IC_{50} ranging from 0. 81 μM to 5.48 μM and 1.41 μM to 6.24 μM, respectively. Compound **7** showed higher antiproliferative activities than SAHA against all tested five human cancer cell lines with the exception of PC-3. Compound **7** proved to be 10-fold more potent than SAHA in the case of MGC-803.

2.5. Western blot analysis

To determine whether target compounds are cell-active LSD1/HDACs dual inhibitors, the effects of selected compound **7** on the methylation levels of LSD1 substrates H3K4 and H3K9 and acetylation levels of H3, the biomarkers of HDACs inhibition, were analyzed. After treatment of MGC-803 cells for 24 h with compound **7** at different concentrations (0, 1.0 and 2.0 μM), the amounts of H3K4me2 and H3K9me2 were dose dependently elevated, while the levels of H3K4me3 was not affected. These results validated that compound **7** is cell-active LSD1 inhibitor (**Fig. 3A**). As expected, exposure to compound **7** also induced a marked acetylation of histone H3 in a dose-dependent manner, suggesting that compound **7** is an effective HDAC inhibitor. It is noteworthy that while the *in vitro* HDACs inhibitory activity of compound **7** was comparable to that of SAHA, compound **7**-induced acetylated histone H3 was more evident (**Fig. 3B**). These results revealed that compound **7** can inhibit LSD1 and HDACs in cells, which were consistent with its strong inhibitory activities against LSD1, HDACs and cancer cells.

2.6. Apoptotic assay

Flow cytometry assay was performed to evaluate the ability of compound **7** to induce apoptosis in MGC-803 cells. Treatment in MGC-803 cells with compound **7** at different concentrations (0, 2.5, 5.0, 7.5 μM) for 24 h, resulted in 4.82%, 26.77%, 37.20% and 42.60% cells apoptosis, respectively (**Fig. 4A**), whereas after treatment with compound **7** (0, 2.5, 5.0, 7.5 μM) for 48 h, the percentage of apoptotic cells were 7.47%, 72.40%, 85.9% and 91.0%, respectively (**Fig. 4B**). The results showed that compound **7** markedly increased the cellular apoptosis in a concentration and time-dependent manner, which might result from concerted inhibition of LSD1 and HDACs activity.

2.7. *Analysis of mitochondrial membrane potential*

Loss of mitochondrial membrane potential (MMP) plays an important role in the apoptotic process and is lethal to the cells. The remarkable apoptosis induced by compound **7** led us to investigate whether this compound had an effect on the MMP. After MGC-803 cells were treated with different concentrations of compound **7** (0, 2.5, 5.0, 7.5 μM) for 48 h, the polarization of the MMP decreased remarkably as compared with the control group in a dose-dependent manner (**Fig.5**). The results showed that compound **7**-induced cellular apoptosis might be mediated via the mitochondrial pathway.

2.8. Docking study

In order to investigate the binding model of compound **7** and LSD1, we carried out molecular docking study adopting the software MOE 2015.10. A co-structure figure of the N-substituted tranylcypromine derivate (GSK2699537) with LSD1 which covalently binds to FAD-C4a (**Fig. 6A**) has been reported in previous study [68], but the X-ray structure is not released in the Protein Data Bank. In this study, compound **7** is a N-substituted tranylcypromine derivative as well as GSK2699537, so we speculate that they have the similar binding mode. Here, the protein LSD1 (PDB ID: 2V1D) containing a free cofactor FAD, H3K4 mimetic peptide as substrate and CoREST as corepressor was selected as the docking receptor. The covalent docking was not supported in the present version of MOE 2015.10, therefore, we used the non-covalent docking method to mimic covalent docking process and the position occupied by substrate was selected as the docking site on the basis of hypothesis of covalently inhibitory mechanism [69] in this study.

In the present study, compound **7** can be successfully docked into the substrate-binding site. Among the top 20 score's conformers, there are two main type conformations. The first type is the one adopting a similar pose to the adduct formed by GSK2699537 with FAD-C4a which occupies more than half of the docking conformations. And all the other docking conformations appears the same type called as the second type which is the one appearing the opposite pose to GSK2699537. Based on the hypothesis of covalently inhibitory mechanism, the first type conformation is considered in the study. Here, the docking pose with the highest score is shown in **Fig. 6B**. The α-C atom of cyclopropylamine moiety situates at a distance of 3.50 Å to FAD-C4a and the N atom of cyclopropylamine moiety is located 5.0Å from the Flavin, according to the covalent inhibitor hypothesis, which tends to form the covalent bond between FAD-C4a and cyclopropane. Meanwhile, hydroxamic acid carbonyl forms a hydrogen bond with Gln358, amine of amide forms a polar contact with Asp556, and amine of tranylcypromine forms salt-bridge with Ala809. Alkyl chain is buried into a hydrophobic pocket surrounded by Phe538, Leu693, Leu536, Phe382, Trp531, Leu677 and Trp695. In addition, the phenyl group connecting with amide is located in the hydrophobic regions which formed by Phe538, Ala539, Tyr761and Ala809, while the cyclopropylamine moiety extensively forms hydrophobic interactions with flavin ring, His564, Val333, Thr335, Thr310, Phe538 and Trp695. All these interactions indicate that compound **7** could well dock into the substrate-binding pocket of LSD1.

Compound **7** was also docked into the active site of HDAC2 to explain its potent inhibitory activity (23nM). Due to compound **7** is quite similar to Vorinostat (SAHA) which was published by Lauffer et al [70], 4LXZ was selected as the docking receptor. The docking conformation with the highest score indicates that compound **7** fits the

active site appropriately (**Fig. 7A**, **B**). The catalytic Zn^{2+} ion situated at the bottom of the active site could form coordinate bonds with Asp181, His183, and Asp269 as well as the carbonyl oxygen of the hydroxamate of compound **7**. Meanwhile, the carbonyl oxygen and amine of the hydroxamic acid moiety have a hydrogen-bond interaction with Tyr308, His146, respectively. The alkyl linker group is located in the narrow lipophilic tube formed by Gly154, Phe155, His183, Phe210 and Leu276, and the amine nitrogen forms a polar contact with Asp104. The cap group can be well accommodated in the hydrophobic groove on the rim of active site of HDAC2 (**Fig.7B**). Besides, the relative long cap group is stabilized by the salt-bridge through amine with Glu103.

2.9 Theoretical evaluation of ADMET properties

Computer predictions of absorption, distribution, metabolism, elimination and toxicity (ADMET) properties of the target compounds was performed utilizing the molinspiration property calculator and preADMET. The results are presented in **Table 4**. All the tested compounds followed Lipinski's rule of 5, indicating that these compounds would not be expected to cause problems with oral bioavailability. Additionally, all the evaluated compounds showed TPSA range 61.4-90.2 Å² (<140 Å²), suggesting good permeability and transport of the compounds in the cellular plasma membrane. The studied compounds are found to be non-carcinogenicity and non-inhibitors of CYP-3A4 and CYP-2C19, which are important enzymes involved in drug metabolism.

3. Conclusions

In conclusion, a series of tranylcypromine derivatives with pharmacophore characteristics of HDACi have been designed, synthesized and evaluated as dual inhibitors against LSD1 and HDACs. Compound **7** displayed the most potent inhibitory activity against HDAC1 and HDAC2 with IC_{50} of 15 nM and 23 nM, respectively. It also showed potent inhibition against LSD1 with IC_{50} of 1.20 μM. Western blotting showed that compound **7** dose-dependently increased the amount of H3ac, H3K4me2 and H3K9me2 in MGC-803, as expected with LSD1/HDACs dual inhibitors. *In vitro* cell growth inhibition assays indicated that compound **7** possessed potent antiproliferative activity with IC_{50} values of 0.81~5.48 μM against five cancer cell lines, and is more potent than SAHA. Compound **7** could induce apoptosis of MGC-803 cells accompanied with decrease of the MMP. Molecular docking of the compound **7** into the active binding sites of LSD1 and HDAC2 was performed and the result suggested that compound **7** could bind well with these two sites. These data support further studies for the rational design of more efficient LSD1/HDACs dual inhibitors for cancer treatment.

4. Experimental section

4.1. Chemistry

4.1.1. General procedures

Reagents and solvents were purchased from commercial sources, when necessary, were purified and dried by standard methods. Melting points were determined on an X-5 micromelting apparatus and are uncorrected. ^{1}H NMR and ^{13}C NMR spectra were recorded on a Bruker Avance III HD 400 MHz and 100 MHz spectrometer at room temperature, using TMS as an internal standard. Chemical shifts were reported in ppm (δ). Spin multiplicities were described as s (singlet), d (doublet), dd (double doublet), t (triplet), br (broad signal), or m (multiplet). Coupling constants were reported in

hertz (Hz). High resolution mass spectrometry (HRMS) was recorded on a Bruker MicrOTOF-Q III Micro mass spectrometer by electrospray ionization (ESI).

4.1.2. General procedure for synthesis of compounds **2** *and* **8**.

To a stirred solution of compound **1** (1.0 equiv) in dry DMF was added NaH (3.0 equiv) and methyl 4-(bromomethyl)benzoate (1.1 equiv) or methyl 3-(4-bromomethyl)cinnamate (1.1 equiv) at 0°C under N_2. The above mixture was stirred for 0.5 h at room temperature. The mixture was diluted with EtOAc and the organic phase was washed with water and brine, dried with anhydrous Na_2SO_4, filtered, concentrated under reduced pressure, and purified by flash column chromatography on silica gel, to afford the pure product **2** and **8**.

4.1.2.1. methyl 4-(((tert-butoxycarbonyl)(2-phenylcyclopropyl)amino)methyl) benzoate (**2**)

Colorless oil, Yield: 67.3%. ^{1}H NMR (400 MHz, $CDCl_3$) δ 7.99 (d, *J* = 8.4 Hz, 2H), 7.30 (d, *J* = 8.0 Hz, 2H), 7.25-7.20 (m, 2H), 7.17-7.13 (m, 1H), 7.03 (d, *J* = 7.6 Hz, 2H), 4.64 (d, *J* = 16.0 Hz, 1H), 4.44 (d, *J* = 16.0 Hz, 1H), 3.91 (s, 3H), 2.71-2.68 (m, 1H), 2.16-2.11 (m, 1H), 1.42 (s, 9H), 1.31-1.25 (m, 1H), 1.18-1.14 (m, 1H). HRMS (ESI) calcd for $C_{23}H_{27}NNaO_4$ $[M + Na]^+$: 404.1832, Found: 404.1833.

4.1.2.2. (E)-methyl 3-(4-(((tert-butoxycarbonyl)(2-phenylcyclopropyl)amino)methyl) phenyl) acrylate (**8**)

Colorless oil, Yield: 71.1%. ^{1}H NMR (400 MHz, $CDCl_3$) δ 7.68 (d, *J* = 16.0 Hz, 1H), 7.47 (d, *J* = 8.0 Hz, 2H), 7.27-7.21 (m, 4H), 7.17-7.13 (m, 1H), 7.04 (d, *J* = 7.2 Hz, 2H), 6.42 (d, *J* = 16.0 Hz, 1H), 4.61 (d, *J* = 14.8 Hz, 1H), 4.39 (d, *J* = 14.8 Hz, 1H), 3.82 (s, 3H), 2.69-2.67 (m, 1H), 2.16-2.12 (m, 1H), 1.43 (s, 9H), 1.31-1.22 (m, 1H), 1.20-1.16 (m, 1H). HRMS (ESI) calcd for $C_{25}H_{29}NNaO_4$ $[M + Na]^+$: 430.1989, Found: 430.1990.

4.1.3. General procedure for synthesis of compounds **3** *and* **9**.

Lithium hydroxide (5.0 equiv) was added to a solution of compound **3** or **9** in THF -H_2O (1:1) and stirred at room temperature for 8-11 h. The mixture pH was adjusted to 2-3 by the addition of 1.0 M hydrochloric acid, and the resultant precipitate was collected by filtration and dried to give compounds **3** and **9**, which was used in the next reaction without further purification.

4.1.3.1. 4-(((tert-butoxycarbonyl)(2-phenylcyclopropyl)amino)methyl)benzoic acid (**3**)

White solid, Yield: 86.7%, Mp:135-136°C. ^{1}H NMR (400 MHz, DMSO-d_6) δ 12.84 (br, 1H), 7.91 (d, *J* = 8.0 Hz, 2H), 7.33 (d, *J* = 8.4 Hz, 2H), 7.25-7.21 (m, 2H), 7.14 (t, *J* = 7.2 Hz, 1H),7.08 (d, *J* = 7.2 Hz, 2H), 4.60 (d, *J* = 16.0 Hz, 1H), 4.41 (d, *J* = 16.0 Hz, 1H), 2.68-2.61 (m, 1H), 2.19-2.14 (m, 1H), 1.34-1.27 (m, 10H), 1.19-1.13 (m, 1H). HRMS (ESI) calcd for $C_{22}H_{25}NNaO_4$ $[M + Na]^+$: 390.1676, Found: 390.1677.

4.1.3.2. (E)-3-(4-(((tert-butoxycarbonyl)(2-phenylcyclopropyl)amino)methyl)phenyl) acrylic acid (**9**)

White solid, Yield: 84.9%, Mp: 146-147°C. ^{1}H NMR (400 MHz, DMSO) δ 12.40 (br, 1H), 7.66 (d, *J* = 8.0 Hz, 2H), 7.57 (d, *J* = 16.0 Hz, 1H), 7.27-7.20 (m, 4H), 7.14 (t, *J*

= 7.2 Hz, 1H), 7.06 (d, *J* = 7.2 Hz, 2H), 6.51 (d, *J* = 16.0 Hz, 1H), 4.56 (d, *J* = 16.0 Hz, 1H), 4.37 (d, *J* = 16.0 Hz, 1H), 2.63-2.59 (m, 1H), 2.17-2.12 (m, 1H), 1.35-1.23 (m, 10H), 1.18-1.13 (m, 1H). HRMS (ESI) calcd for $C_{24}H_{27}NNaO_4$ $[M + Na]^+$: 416.1832, Found: 416.1831.

4.1.4. General procedure for synthesis of compounds **4** *and* **10**.

Triethylamine (3.0 equiv) was added to a solution of compounds **3** (1.0 equiv) or **9** (1.0 equiv) and HBTU (1.5 equiv) in dry DMF at 0°C under nitrogen. After the mixture was stirred for 0.5 h, appropriate amino-compounds (1.5 equiv) was added and stirred for additional 12 h at room temperature. The mixture was diluted with EtOAc and the organic phase was washed with water and brine, dried over anhydrous Na_2SO_4, concentrated under reduced pressure, and purified by flash column chromatography on silica gel, to afford the pure product **4** and **10**.

4.1.4.1. tert-butyl 4-(hydroxycarbamoyl)benzyl(2-phenylcyclopropyl)carbamate (**4a**)
Yellowish solid, Yield: 54.6%, Mp:185-186°C.^{1}H NMR (400 MHz, DMSO-d_6) δ 11.18 (s, 1H), 9.03 (s, 1H), 7.71 (d, *J* = 8.0 Hz, 2H), 7.28 (d, *J* = 8.0 Hz, 2H), 7.25-7.21 (m, 2H), 7.14 (t, *J* = 7.2 Hz, 1H), 7.08 (d, *J* = 7.2 Hz, 2H), 4.57 (d, *J* = 16.4 Hz, 1H), 4.38 (d, *J* = 16.4 Hz, 1H), 2.65-2.61 (m, 1H), 2.18-2.12 (m, 1H), 1.34-1.23 (m, 10H), 1.18-1.11 (m, 1H). HRMS (ESI) calcd for $C_{22}H_{26}N_2NaO_4$ $[M+Na]^+$: 405.1785, Found: 405.1787.

4.1.4.2. tert-butyl4-((2-((tert-butoxycarbonyl)amino)phenyl)carbamoyl)benzyl(2-phenylcyclopropyl)carbamate (**4b**)
White solid, Yield: 69.1%, Mp:68-69°C. ^{1}H NMR (400 MHz, DMSO-d_6) δ 9.81 (s, 1H), 8.72 (s, 1H), 7.92 (d, *J* = 8.0 Hz, 2H), 7.55-7.51 (m, 2H), 7.37 (d, *J* = 8.0 Hz, 2H), 7.26-7.08 (m, 7H), 4.62 (d, *J* = 16.0 Hz, 1H), 4.44 (s, *J* = 16.0 Hz, 1H), 2.66-2.60 (m, 1H), 2.20-2.14 (m, 1H), 1.44 (s, 9H), 1.36-1.23 (m, 10H), 1.23-1.15 (m, 1H). HRMS (ESI) calcd for $C_{33}H_{39}N_3NaO_5$ $[M+Na]^+$: 580.2782, Found: 580.2783.

4.1.4.3. methyl 7-(4-(((tert-butoxycarbonyl)(2-phenylcyclopropyl)amino)methyl) benzamido)heptanoate (**4c**)
Colorless oil, Yield 61.2%. ^{1}H NMR (400 MHz, DMSO-d_6) δ 8.40 (t, *J* = 5.6 Hz, 1H), 7.79 (d, *J* = 8.0 Hz, 2H), 7.28 (d, *J* = 8.0 Hz, 2H), 7.25-7.21 (m, 2H), 7.14 (t, *J* = 7.6 Hz, 1H), 7.07 (d, *J* = 7.6 Hz, 2H), 4.57 (d, *J* = 16.0 Hz, 1H), 4.39 (d, *J* = 16.0 Hz, 1H), 3.57 (s, 3H), 3.23 (q, *J* = 6.4 Hz, 2H), 2.64-2.59 (m, 1H), 2.29 (t, *J* = 7.6 Hz, 2H), 2.18-2.12 (m, 1H), 1.54-1.48 (m, 4H), 1.34 (s, 9H), 1.31-1.24 (m, 5H), 1.18-1.13 (m, 1H). HRMS (ESI) calcd for $C_{30}H_{40}N_2NaO_5$ $[M+Na]^+$: 531.2829, Found: 531.2834.

4.1.4.4.(E)-tert-butyl4-(3-(hydroxyamino)-3-oxoprop-1-en-1-yl)benzyl(2-phenylcyclopropyl)carbamate (**10a**)
White solid, Yield: 52.3%, Mp:137-138 °C.^{1}H NMR (400 MHz, DMSO-d_6) δ 10.76 (s, 1H), 9.04 (s, 1H), 7.53 (d, *J* = 8.0 Hz, 2H), 7.43 (d, *J* = 16.0 Hz, 1H), 7.26-7.21 (m, 4H), 7.14 (t, *J* = 7.6 Hz, 1H), 7.08 (d, *J* = 7.6 Hz, 2H), 6.44 (d, *J* = 16.0 Hz, 1H), 4.55 (d, *J* = 16.0 Hz, 1H), 4.36 (d, *J* = 16.0 Hz, 1H), 2.63-2.59 (m, 1H), 2.17-2.12 (m, 1H), 1.35-1.27 (s, 10H), 1.19-1.13 (m, 1H). HRMS (ESI) calcd for $C_{24}H_{28}N_2NaO_4$ $[M + Na]^+$: 431.1941, Found: 431.1946.

4.1.4.5. (E)-tert-butyl 4-(3-((2-((tert-butoxycarbonyl)amino)phenyl)amino)-3-

oxoprop-1-en-1-yl)benzyl(2-phenylcyclopropyl)carbamate (**10b**)
White solid, Yield: 70.7%, Mp: 83-84°C.^{1}H NMR (400 MHz, $CDCl_3$) δ 8.26 (br, 1H), 7.75 (d, *J* = 15.6 Hz, 1H), 7.63 (br, 1H), 7.49-7.40 (m, 3H), 7.27-7.16 (m, 7H), 7.06 (d, *J* = 7.8 Hz, 2H), 6.91 (br, 1H), 6.53 (d, *J* = 15.6 Hz, 1H), 4.64 (d, *J* = 16.0 Hz, 1H), 4.43 (d, *J* = 16.0 Hz, 1H), 2.72-2.67 (m, 1H), 2.17-2.13 (m, 1H), 1.53 (s, 9H), 1.43 (s, 9H), 1.33-1.26 (m, 1H), 1.24-1.16 (m, 1H). HRMS (ESI) calcd for $C_{35}H_{41}N_3NaO_5$ $[M + Na]^+$: 606.7064, Found: 606.7062.

4.1.5 . Procedure for synthesis of tert-butyl 4-((7-(hydroxyamino)-7-oxoheptyl) carbamoyl)benzyl(2-phenylcyclopropyl)carbamate (**6**)

KOH (2.8g, 50.9mmol) and $NH_2OH{\cdot}HCl$ (2.34g, 34.3mmol) were dissolved, respectively, in 7 mL and 12 mL MeOH to get solution A and solution B. Next solution A was added dropwise to solution B. After filtering the precipitate (KCl), a mix solution of NH_2OK and NH_2OH was obtained. Compound **4c** (0.254 g, 0.5 mmol) was dissolved in 5mL NH_2OK solution and stirred overnight. After the reaction was complete, it was evaporated under vacuum. The residue was acidified with 1 N HCl to a pH 3-4 and then extracted with EtOAc. The organic layer was washed with brine and dried over Na_2SO_4 overnight. The crude material was purified via flash chromatography to afford the compound **6** (104 mg, yield 41.1%). White solid, Mp: 61-62°C. ^{1}H NMR (400 MHz, DMSO) δ 10.35 (s, 1H), 8.67 (s, 1H), 8.40 (t, *J* = 5.6 Hz, 1H), 7.80 (d, *J* = 8.0 Hz, 2H), 7.29 (d, *J* = 8.4 Hz, 2H), 7.23-7.21 (m, 2H), 7.14 (t, *J* = 7.2 Hz, 1H), 7.08 (d, *J* = 7.2 Hz, 2H), 4.57 (d, *J* = 16.0 Hz, 1H), 4.40 (d, *J* = 16.0 Hz, 1H), 3.23 (q, *J* = 6.4 Hz, 2H), 2.64-2.60 (m, 1H), 2.16-2.12 (m, 1H), 1.94 (t, *J* = 7.2 Hz, 2H), 1.51-1.48 (m, 4H), 1.35 (s, 9H), 1.30-1.23 (m, 5H), 1.18-1.13 (m, 1H). HRMS (ESI) calcd for $C_{29}H_{40}N_3O_5$ $[M + H]^+$: 510.2962, Found: 510.2965.

4.1.6. General procedure for synthesis of compounds **5**, **7** *and* **11**.
CF_3COOH (20 equiv) was added to a solution of compounds **4a-b**, **6** or **10** (1.0 equiv) in CH_2Cl_2 at 0°C. The reaction mixture was warmed to room temperature and stirred at the same temperature. Upon completion, the mixture was concentrated under vacuum; the residue was dissolved in CH_2Cl_2, washed with saturated $NaHCO_3$ and brine, dried over anhydrous Na_2SO_4, concentrated under vacuum, and purified by flash column chromatography on silica gel, to afford the pure product.

4.1.6.1. N-hydroxy-4-(((2-phenylcyclopropyl)amino)methyl)benzamide (**5a**)
Yellowish solid, Yield: 74.1%, Mp:103-104°C. ^{1}H NMR (400 MHz, DMSO-d_6) δ 11.26 (br, 1H), 9.03 (br, 1H), 7.70 (d, *J* = 8.0 Hz, 2H), 7.38 (d, *J* = 8.0 Hz, 2H), 7.22-7.18 (m, 2H), 7.10 (t, *J* = 7.2 Hz, 1H), 6.97 (d, *J* = 7.2 Hz, 2H), 3.83 (s, 2H), 2.27-2.19 (m, 1H), 1.87 (s, 1H), 1.07-1.02 (m, 1H), 0.97-0.92 (m, 1H). HRMS (ESI) calcd for $C_{17}H_{19}N_2O_2$ $[M + H]^+$: 283.1441, Found: 283.1443.

4.1.6.2. N-(2-aminophenyl)-4-(((2-phenylcyclopropyl)amino)methyl)benzamide (**5b**)
White solid, Yield: 77.4%, Mp:115-116°C. ^{1}H NMR (400 MHz, DMSO-d_6) δ 9.64 (s, 1H), 7.92 (d, *J* = 8.0 Hz, 2H), 7.44 (d, *J* = 8.4 Hz, 2H), 7.23-7.15 (m, 3H), 7.10 (t, *J* = 7.2 Hz, 1H), 7.00-6.95 (m, 3H), 6.79 (dd, *J* = 8.0, 1.2 Hz, 1H), 6.60 (t, *J* = 7.2 Hz, 1H), 4.90 (s, 2H), 3.85 (s, 2H), 3.06 (br, 1H), 2.23-2.19 (m, 1H), 1.88-1.83 (m, 1H), 1.06-1.01 (m, 1H), 0.97-0.92 (m, 1H). ^{13}C NMR (101 MHz, DMSO-d_6) δ 165.64, 145.10, 143.62, 142.96, 133.25, 128.56, 128.18, 128.08, 127.15, 126.90, 125.97,

125.58, 123.89, 116.74, 116.61, 52.73, 42.06, 25.00, 17.25. HRMS (ESI) calcd for $C_{23}H_{23}N_3NaO$ $[M + Na]^+$: 380.1733, Found: 380.1734.

4.1.6.3. N-(7-(hydroxyamino)-7-oxoheptyl)-4-(((phenylcyclopropyl)amino)methyl) Benzamide (**7**)
White solid, Yield: 68.6%, Mp:140-141°C. ^{1}H NMR (400 MHz, DMSO-d_6) δ 10.34 (s, 1H), 8.66 (s, 1H), 8.37 (t, *J* = 5.6 Hz, 1H), 7.76 (d, *J* = 8.0 Hz, 2H), 7.37 (d, *J* = 8.0 Hz, 2H), 7.21-7.17 (m, 2H), 7.11-7.07 (m, 1H), 6.96 (d, *J* = 6.8 Hz, 2H), 3.80 (s, 2H), 3.22 (q, *J* = 6.8 Hz, 2H), 2.96 (s, 1H), 2.21-2.17 (m, 1H), 1.94 (t, *J* = 7.2 Hz, 2H), 1.85-1.80 (m, 1H), 1.52-1.46 (m, 4H), 1.29-1.25 (m, 4H), 1.03-0.98 (m, 1H), 0.95-0.90 (m, 1H). ^{13}C NMR (101 MHz, DMSO) δ 169.55, 166.38, 144.56, 142.94, 133.38, 128.52, 128.13, 127.41, 125.94, 125.55, 52.73, 42.08, 32.71, 29.53, 28.83, 26.71, 25.57, 24.99, 17.23. RMS (ESI) calcd for $C_{24}H_{31}N_3NaO_3$[M + Na]$^+$: 432.2258, Found: 432.2262.

4.1.6.4. (E)-N-hydroxy-3-(4-(((2-phenylcyclopropyl)amino)methyl)phenyl)acrylamide (**11a**)
White solid, Yield: 57.7%, Mp:125-126°C. ^{1}H NMR (400 MHz, DMSO-d_6) δ 10.90 (br, 1H), 9.07 (br, 1H), 7.47 (d, *J* = 7.8 Hz, 2H), 7.42 (d, *J* = 16.0 Hz, 1H), 7.34 (d, *J* = 7.8 Hz, 2H), 7.21-7.17 (m, 2H), 7.09 (t, *J* = 7.2 Hz, 1H), 6.97 (d, *J* = 7.2 Hz, 2H), 6.50 (d, *J* = 16.0 Hz, 1H), 3.77 (s, 2H), 2.96 (br, 1H), 2.21-2.17 (m, 1H), 1.84-1.79 (m, 1H), 1.03-0.98 (m, 1H), 0.95-0.90 (m, 1H). ^{13}C NMR (101 MHz, DMSO) δ 163.25, 143.04, 142.97, 138.49, 133.60, 128.95, 128.53, 127.70, 125.93, 125.55, 119.01, 52.80, 42.12, 25.02, 17.21. HRMS (ESI) calcd for $C_{19}H_{20}N_2NaO_2$ $[M + Na]^+$: 331.1417, Found: 331.1419.

4.1.6.5. (E)-N-(2-aminophenyl)-3-(4-(((2-phenylcyclopropyl)amino)methyl)phenyl) acryl Amide (**11b**)
White solid, Yield: 69.2%, Mp:142-143°C. ^{1}H NMR (400 MHz, DMSO-d_6) δ 9.36 (s, 1H), 7.55-7.51 (m, 3H), 7.38-7.33 (m, 3H), 7.22-7.18 (m, 2H), 7.09 (t, *J* = 7.2 Hz, 1H), 6.98-6.85 (m, 4H), 6.75 (dd, *J* = 8.4, 1.6 Hz, 1H), 6.58 (td, *J* = 7.6, 1.2 Hz, 1H), 4.95 (s, 2H), 3.79 (s, 2H), 3.00 (br, 1H), 2.23-2.19 (m, 1H), 1.85-1.80 (m, 1H), 1.04-0.99 (m, 1H), 0.96-0.91 (m, 1H). ^{13}C NMR (101 MHz, DMSO) δ 164.03, 143.29, 142.95, 142.05, 139.97, 133.62, 129.02, 128.53, 127.89, 126.20, 125.95, 125.56, 125.14, 124.00, 122.07, 116.73, 116.46, 52.83, 42.15, 25.05, 17.22. HRMS (ESI) calcd for $C_{25}H_{26}N_3O$ $[M + H]^+$: 384.2070, Found: 384.2072.

4.2. LSD1, MAO-A and MAO-B inhibition assays

Inhibitory effects of the candidate compounds against LSD1, MAO-A and MAO-B were evaluated following our previous method [31]. In brief, the candidate compounds were incubated with the recombinant LSD1 and H3K4me2. After that, the fluorescence was measured at excitation wavelength 530 nm and emission wavelength 590 nm with the addition of Amplex Red and horseradish peroxidase (HRP) in order to evaluate the inhibition rate of the candidate compound. MAO inhibitory activities were determined using a commercialized MAO-Glo assay kit from Promega, according to the manufacturer's protocol.

4.3. HDAC inhibition assay

In vitro HDAC1 (BPS, Cat. No.50051), HDAC2 (BPS, Cat. No.50002) and HDAC5 (BPS, Cat. No.50005) assays were carried out by Shanghai Chempartner Co., Ltd in Shanghai, China, using SAHA (Sigma, Cat. No. SML0061) as the reference compound for HDAC1 and HDAC2, and TMP269 (MCE, Cat. No. HY-18360) as the reference compound for HDAC5. Those compounds were tested over 10 serial concentrations, 100 μM starting with 3-fold dilution. The general procedures were as the following: 1x assay buffer (modified Tris Buffer) was prepared, and candidate compounds were transferred to assay plate by Echo550 in 100% DMSO. Substrate solution was made by preparing enzyme solution in 1x assay buffer and adding trypsin and Ac-peptide substrate in 1x assay buffer. 15μL of enzyme solution or 1x assay buffer was transferred to assay plate or for low control and incubated at room temperature for 15 min. Substrate solution (10 μL) was then added to each well to start reaction. The plates were incubated at room temperature for 60 min to allow the fluorescence signal to develop. The fluorescence generated was monitored with excitation at 355 nm and emission at 460 nm on an Synergy MX.

4.4. Anti-proliferative activity assays

Exponentially growing cells were seeded into 96-well plates at a concentration of 5×10^3 cells per well. After 24 h incubation at 37°C, the culture medium was removed and replaced with fresh medium containing appropriate concentrations of each test compound. The cells were incubated for another 72 h at 37°C in 5% CO_2. Afterward, 20μL of MTT solution (5 mg/mL) was added to all wells and incubated for 4 h at 37°C. Then, the supernatant was discarded and 150 mL of DMSO was added to dissolve the formazan product; the absorbance was measured using a microplate reader at a wavelength of 490 nm. Each concentration was analyzed in triplicate and the experiment was repeated three times. The average 50% inhibitory concentration (IC_{50}) was determined from the dose-response curves according to the inhibition ratio for each concentration.

4.5. Flow cytometric analysis of cellular apoptosis

MGC-803 cells (5.0×10^4) were plated in 6-well plates and treated with increasing doses (0, 2.5, 5.0 and 7.5 μM) of compound **7** at 37°C for 24 h or 48h. Cells were then harvested and the Annexin-V-FITC/PI apoptosis kit (Biovision) was used according to the manufacturer's protocol to detect apoptotic cells. Ten thousand events were collected for each sample and analyzed by Accuri C6 flow cytometer.

4.6. Detection of mitochondrial membrane potential

Mitochondria membrane potential was determined by the fluorescent dye JC-1. After treatment with different concentrations of compound **7** under standard culture conditions for 48 h, the cells were stained with 10 mg/mL JC-1 and incubated under standard conditions for 30 min. The fluorescence intensity of cells was determined by flow cytometry.

4.7. Western Blot

10^6 MGC-803 cells/well were incubated with compound **7** (0, 1.0, 2.0 μM) or SAHA (2.0 μM) for 2 days. Histone proteins were extracted using EpiQuik total histone extraction kit (Epigentek) according to the manufacturer's protocol. Equivalent

amounts of cell lysates were denatured, separated by SDS-PAGE and transferred onto nitrocellulose membranes. After blocking with PBS containing 5% nonfat milk, the membranes were incubated overnight at 4°C with specific primary antibodies, followed by incubation with appropriate secondary antibodies. The immunoblots were visualized by enhanced chemiluminescence detection kit from Thermo Fisher.

4.8. Molecular Docking

All molecular modeling studies were performed with MOE (The Molecular Operating Environment) Version 2015.10. The crystal structure for LSD1 (PDB code: 4LXZ) and HDAC2 (PDB code: 4LXZ) were obtained from the RCSB protein data bank. The docking procedure contained the preparation of protein and ligand and the operation of docking. The preparation of protein structure was performed using the Quickprep module, which contained the deletion of waters, the addition of hydrogen atoms, the protonation and the repair of missing residues. The geometry optimization of ligand structure mainly was executed by energy minimization and conformation search. Next, compound **7** was docked into the LSD1 or HDAC2. Default triangle matcher method was used for placement of ligand and the final conformation was scored by GBVI/WSA dG. All these above treatments were formed in Amber 10: EHT forcefield.

Acknowledgments
We are grateful for the financial support from the National Natural Science Foundation of China Project (No. 81402793 for Ying-Chao Duan, No. 81502952 for Yong-Cheng Ma and No. 21403200 for Li-Na Ding).

[1] L. Ellis, P.W. Atadja, R.W. Johnstone, Epigenetics in cancer: targeting chromatin modifications, Mol Cancer Ther, 8 (2009) 1409-1420.
[2] A.D. Kelly, J.J. Issa, The promise of epigenetic therapy: reprogramming the cancer epigenome, Curr Opin Genet Dev, 42 (2017) 68-77.
[3] S.J. Conway, P.M. Woster, W.J. Greenlee, G. Georg, S. Wang, Epigenetics: Novel Therapeutics Targeting Epigenetics, J Med Chem, 59 (2016) 1247-1248.
[4] F. Perri, F. Longo, M. Giuliano, F. Sabbatino, G. Favia, F. Ionna, R. Addeo, G. Della Vittoria Scarpati, G. Di Lorenzo, S. Pisconti, Epigenetic control of gene expression: Potential implications for cancer treatment, Crit Rev Oncol Hematol, 111 (2017) 166-172.
[5] C.H. Arrowsmith, C. Bountra, P.V. Fish, K. Lee, M. Schapira, Epigenetic protein families: a new frontier for drug discovery, Nat Rev Drug Discov, 11 (2012) 384-400.
[6] Y. Shi, F. Lan, C. Matson, P. Mulligan, J.R. Whetstine, P.A. Cole, R.A. Casero, Y. Shi, Histone demethylation mediated by the nuclear amine oxidase homolog LSD1, Cell, 119 (2004) 941-953.
[7] Y.J. Shi, C. Matson, F. Lan, S. Iwase, T. Baba, Y. Shi, Regulation of LSD1 histone demethylase activity by its associated factors, Mol Cell, 19 (2005) 857-864.
[8] E. Metzger, M. Wissmann, N. Yin, J.M. Muller, R. Schneider, A.H. Peters, T. Gunther, R. Buettner, R. Schule, LSD1 demethylates repressive histone marks to promote androgen-receptor-dependent transcription, Nature, 437 (2005) 436-439.
[9] J. Huang, R. Sengupta, A.B. Espejo, M.G. Lee, J.A. Dorsey, M. Richter, S. Opravil, R. Shiekhattar, M.T. Bedford, T. Jenuwein, S.L. Berger, p53 is regulated by the lysine demethylase LSD1, Nature, 449 (2007) 105-108.

[10] J. Wang, S. Hevi, J.K. Kurash, H. Lei, F. Gay, J. Bajko, H. Su, W. Sun, H. Chang, G. Xu, F. Gaudet, E. Li, T. Chen, The lysine demethylase LSD1 (KDM1) is required for maintenance of global DNA methylation, Nat Genet, 41 (2009) 125-129.
[11] H. Kontaki, I. Talianidis, Lysine methylation regulates E2F1-induced cell death, Mol Cell, 39 (2010) 152-160.
[12] S. Hayami, J.D. Kelly, H.S. Cho, M. Yoshimatsu, M. Unoki, T. Tsunoda, H.I. Field, D.E. Neal, H. Yamaue, B.A. Ponder, Y. Nakamura, R. Hamamoto, Overexpression of LSD1 contributes to human carcinogenesis through chromatin regulation in various cancers, Int J Cancer, 128 (2011) 574-586.
[13] C.A. Stewart, L.A. Byers, Altering the Course of Small Cell Lung Cancer: Targeting Cancer Stem Cells via LSD1 Inhibition, Cancer Cell, 28 (2015) 4-6.
[14] D.P. Mould, A.E. McGonagle, D.H. Wiseman, E.L. Williams, A.M. Jordan, Reversible inhibitors of LSD1 as therapeutic agents in acute myeloid leukemia: clinical significance and progress to date, Med Res Rev, 35 (2015) 586-618.
[15] W.J. Harris, X. Huang, J.T. Lynch, G.J. Spencer, J.R. Hitchin, Y. Li, F. Ciceri, J.G. Blaser, B.F. Greystoke, A.M. Jordan, C.J. Miller, D.J. Ogilvie, T.C. Somervaille, The histone demethylase KDM1A sustains the oncogenic potential of MLL-AF9 leukemia stem cells, Cancer Cell, 21 (2012) 473-487.
[16] Shixian Lian, Y.S. , Houbao Liu,, J.H. , W.L. , Y.Z. , J.Z. Ying Jiang, Lysine-specific demethylase 1 promotes tumorigenesis and predicts prognosis in gallbladder cancer, Oncotarget, 6 (2015) 33065-33076.
[17] J. Ding, Z.M. Zhang, Y. Xia, G.Q. Liao, Y. Pan, S. Liu, Y. Zhang, Z.S. Yan, LSD1-mediated epigenetic modification contributes to proliferation and metastasis of colon cancer, Br J Cancer, 109 (2013) 994-1003.
[18] S. Lim, A. Janzer, A. Becker, A. Zimmer, R. Schule, R. Buettner, J. Kirfel, Lysine-specific demethylase 1 (LSD1) is highly expressed in ER-negative breast cancers and a biomarker predicting aggressive biology, Carcinogenesis, 31 (2010) 512-520.
[19] T. Murray-Stewart, P.M. Woster, R.A. Casero, Jr., The re-expression of the epigenetically silenced e-cadherin gene by a polyamine analogue lysine-specific demethylase-1 (LSD1) inhibitor in human acute myeloid leukemia cell lines, Amino Acids, 46 (2014) 585-594.
[20] S.K. Sharma, Y. Wu, N. Steinbergs, M.L. Crowley, A.S. Hanson, R.A. Casero, P.M. Woster, (Bis)urea and (bis)thiourea inhibitors of lysine-specific demethylase 1 as epigenetic modulators, J Med Chem, 53 (2010) 5197-5212.
[21] W.J.H.T.C.P.S. James T Lynch, LSD1 inhibition: A therapeutic strategy in cancer?, Expert Opin. Ther. Targets, (2012) 1239-1249.
[22] J.W. Hojfeldt, K. Agger, K. Helin, Histone lysine demethylases as targets for anticancer therapy, Nat Rev Drug Discov, 12 (2013) 917-930.
[23] S. Hazeldine, B. Pachaiyappan, N. Steinbergs, S. Nowotarski, A.S. Hanson, R.A. Casero, Jr., P.M. Woster, Low molecular weight amidoximes that act as potent inhibitors of lysine-specific demethylase 1, J Med Chem, 55 (2012) 7378-7391.
[24] F. Wu, C. Zhou, Y. Yao, L. Wei, Z. Feng, L. Deng, Y. Song, 3-(Piperidin-4-ylmethoxy)pyridine Containing Compounds Are Potent Inhibitors of Lysine Specific Demethylase 1, J Med Chem, 59 (2016) 253-263.
[25] V. Sorna, E.R. Theisen, B. Stephens, S.L. Warner, D.J. Bearss, H. Vankayalapati, S. Sharma, High-Throughput Virtual Screening Identifies NovelN′-(1-Phenylethylidene)-benzohydrazides as Potent, Specific, and Reversible LSD1 Inhibitors, Journal of Medicinal Chemistry, 56 (2013) 9496-9508.

[26] L. Sartori, C. Mercurio, F. Amigoni, A. Cappa, G. Faga, R. Fattori, E. Legnaghi, G. Ciossani, A. Mattevi, G. Meroni, L. Moretti, V. Cecatiello, S. Pasqualato, A. Romussi, F. Thaler, P. Trifiro, M. Villa, S. Vultaggio, O.A. Botrugno, P. Dessanti, S. Minucci, E. Zagarri, D. Carettoni, L. Iuzzolino, M. Varasi, P. Vianello, Thieno[3,2-b]pyrrole-5-carboxamides as New Reversible Inhibitors of Histone Lysine Demethylase KDM1A/LSD1. Part 1: High-Throughput Screening and Preliminary Exploration, J Med Chem, 60 (2017) 1673-1692.
[27] T.E. McAllister, K.S. England, R.J. Hopkinson, P.E. Brennan, A. Kawamura, C.J. Schofield, Recent Progress in Histone Demethylase Inhibitors, J Med Chem, 59 (2016) 1308-1329.
[28] G. Stazi, C. Zwergel, S. Valente, A. Mai, LSD1 inhibitors: a patent review (2010-2015), Expert Opin Ther Pat, 26 (2016) 565-580.
[29] X. Wang, B. Huang, T. Suzuki, X. Liu, P. Zhan, Medicinal chemistry insights in the discovery of novel LSD1 inhibitors, Epigenomics, 7 (2015) 1379-1396.
[30] Y.C. Zheng, J. Ma, Z. Wang, J. Li, B. Jiang, W. Zhou, X. Shi, X. Wang, W. Zhao, H.M. Liu, A Systematic Review of Histone Lysine-Specific Demethylase 1 and Its Inhibitors, Med Res Rev, 35 (2015) 1032-1071.
[31] Y.C. Zheng, Y.C. Duan, J.L. Ma, R.M. Xu, X. Zi, W.L. Lv, M.M. Wang, X.W. Ye, S. Zhu, D. Mobley, Y.Y. Zhu, J.W. Wang, J.F. Li, Z.R. Wang, W. Zhao, H.M. Liu, Triazole-dithiocarbamate based selective lysine specific demethylase 1 (LSD1) inactivators inhibit gastric cancer cell growth, invasion, and migration, J Med Chem, 56 (2013) 8543-8560.
[32] Y.C. Duan, Y.Y. Guan, X.Y. Zhai, L.N. Ding, W.P. Qin, D.D. Shen, X.Q. Liu, X.D. Sun, Y.C. Zheng, H.M. Liu, Discovery of resveratrol derivatives as novel LSD1 inhibitors: Design, synthesis and their biological evaluation, Eur J Med Chem, 126 (2017) 246-258.
[33] Y.C. Duan, Y.C. Ma, E. Zhang, X.J. Shi, M.M. Wang, X.W. Ye, H.M. Liu, Design and synthesis of novel 1,2,3-triazole-dithiocarbamate hybrids as potential anticancer agents, Eur J Med Chem, 62 (2013) 11-19.
[34] S. Valente, V. Rodriguez, C. Mercurio, P. Vianello, B. Saponara, R. Cirilli, G. Ciossani, D. Labella, B. Marrocco, D. Monaldi, G. Ruoppolo, M. Tilset, O.A. Botrugno, P. Dessanti, S. Minucci, A. Mattevi, M. Varasi, A. Mai, Pure enantiomers of benzoylamino-tranylcypromine: LSD1 inhibition, gene modulation in human leukemia cells and effects on clonogenic potential of murine promyelocytic blasts, Eur J Med Chem, 94 (2015) 163-174.
[35] Y. C. Zheng, B. Yu, G. Z. Jiang, X. J. Feng, P. X. He, X. Y. Chu, W. Zhao, H. M. Liu, Irreversible LSD1 Inhibitors: Application of Tranylcypromine and Its Derivatives in Cancer Treatment, Current Topics in Medicinal Chemistry, 16 (2016) 2179-2188.
[36] Phase I Dose Escalation Study of GSK2879552 in Subjects With Acute Myeloid Leukemia (AML), in, ClinicalTrials.gov, https://clinicaltrials.gov/show/NCT02177812A
[37] L. Morera, M. Lubbert, M. Jung, Targeting histone methyltransferases and demethylases in clinical trials for cancer therapy, Clin Epigenetics, 8 (2016) 57.
[38] S.C. Kim, R. Sprung, Y. Chen, Y. Xu, H. Ball, J. Pei, T. Cheng, Y. Kho, H. Xiao, L. Xiao, N.V. Grishin, M. White, X.J. Yang, Y. Zhao, Substrate and functional diversity of lysine acetylation revealed by a proteomics survey, Mol Cell, 23 (2006) 607-618.
[39] G.P. Delcuve, D.H. Khan, J.R. Davie, Roles of histone deacetylases in epigenetic regulation: emerging paradigms from studies with inhibitors, Clin Epigenetics, 4 (2012) 1-13.

[40] E. Verdin, M. Ott, 50 years of protein acetylation: from gene regulation to epigenetics, metabolism and beyond, Nat Rev Mol Cell Biol, 16 (2015) 258-264.
[41] A.H.V.G. Annemieke J. M. DE RUIJTER, Huib N. CARON, Stephan KEMP and Andre B. P. VAN KUILENBURG1, Histone deacetylases (HDACs): characterization of the classical HDAC family, Biochem. J, 370 (2003) 737-749.
[42] R.A.R. Paul A.Marks, Victoria M. Richon, Ronald BreslowThomas Miller and William K.Kelly, Histone deacetylases and cancer: causes and therapies, Nat. Rev. Cancer, 1 (2002) 194-202.
[43] M. Haberland, R.L. Montgomery, E.N. Olson, The many roles of histone deacetylases in development and physiology: implications for disease and therapy, Nat Rev Genet, 10 (2009) 32-42.
[44] M. Manal, M.J. Chandrasekar, J. Gomathi Priya, M.J. Nanjan, Inhibitors of histone deacetylase as antitumor agents: A critical review, Bioorg Chem, 67 (2016) 18-42.
[45] B.S. Mann, J.R. Johnson, M.H. Cohen, R. Justice, R. Pazdur, FDA approval summary: vorinostat for treatment of advanced primary cutaneous T-cell lymphoma, Oncologist, 12 (2007) 1247-1252.
[46] C. Campas-Moya, Romidepsin for the treatment of cutaneous T-cell lymphoma, Drugs Today (Barc), 45 (2009) 787-795.
[47] C.A. Thompson, Belinostat approved for use in treating rare lymphoma, Am J Health Syst Pharm, 71 (2014) 1328.
[48] K.P. Garnock-Jones, Panobinostat: first global approval, Drugs, 75 (2015) 695-704.
[49] Q.-J.Y. De-Si Pan, Xin Fu, Song Shan, Jing-Zhong Zhu, Kun Zhang, Zhi-Bin Li, Zhi-Qiang Ning and Xian-Ping Lu, Discovery of an orally active subtype-selective HDAC inhibitor, chidamide, as an epigenetic modulator for cancer treatment, Med. Chem.Commun, 5 (2014) 1789-1796.
[50] S.V. Clemens Zwergel, Claus Jacob, Antonello Mai, Emerging approaches for histone deacetylase inhibitor drug discovery, Expert Opin. Drug Discov, 10 (2015) 599-613.
[51] A.C. West, R.W. Johnstone, New and emerging HDAC inhibitors for cancer treatment, J Clin Invest, 124 (2014) 30-39.
[52] R. Pathania, S. Ramachandran, G. Mariappan, P. Thakur, H. Shi, J.H. Choi, S. Manicassamy, R. Kolhe, P.D. Prasad, S. Sharma, B.L. Lokeshwar, V. Ganapathy, M. Thangaraju, Combined Inhibition of DNMT and HDAC Blocks the Tumorigenicity of Cancer Stem-like Cells and Attenuates Mammary Tumor Growth, Cancer Res, 76 (2016) 3224-3235.
[53] K.F. Whitecross, A.E. Alsop, L.A. Cluse, A. Wiegmans, K.M. Banks, C. Coomans, M.J. Peart, A. Newbold, R.K. Lindemann, R.W. Johnstone, Defining the target specificity of ABT-737 and synergistic antitumor activities in combination with histone deacetylase inhibitors, Blood, 113 (2009) 1982-1991.
[54] M.C. Chen, C.H. Chen, J.C. Wang, A.C. Tsai, J.P. Liou, S.L. Pan, C.M. Teng, The HDAC inhibitor, MPT0E028, enhances erlotinib-induced cell death in EGFR-TKI-resistant NSCLC cells, Cell Death Dis, 4 (2013) e810.
[55] P.A. Marks, The clinical development of histone deacetylase inhibitors as targeted anticancer drugs, Expert Opin. Investig. Drugs, 19 (2010) 1049-1056.
[56] R.A. Juergens, J. Wrangle, F.P. Vendetti, S.C. Murphy, M. Zhao, B. Coleman, R. Sebree, K. Rodgers, C.M. Hooker, N. Franco, B. Lee, S. Tsai, I.E. Delgado, M.A. Rudek, S.A. Belinsky, J.G. Herman, S.B. Baylin, M.V. Brock, C.M. Rudin,

Combination epigenetic therapy has efficacy in patients with refractory advanced non-small cell lung cancer, Cancer Discov, 1 (2011) 598-607.
[57] Z.K. Eihab Abdelfatah, Nainika Nanda and Nita Ahuja, Epigenetic therapy in gastrointestinal cancer: the right combination, Therapeutic Advances in Gastroenterology, 9 (2016) 560-579.
[58] Y. Wang, H. Zhang, Y. Chen, Y. Sun, F. Yang, W. Yu, J. Liang, L. Sun, X. Yang, L. Shi, R. Li, Y. Li, Y. Zhang, Q. Li, X. Yi, Y. Shang, LSD1 is a subunit of the NuRD complex and targets the metastasis programs in breast cancer, Cell, 138 (2009) 660-672.
[59] D.A. Nalawansha, M.K. Pflum, LSD1 Substrate Binding and Gene Expression Are Affected by HDAC1-Mediated Deacetylation, ACS Chem Biol, 12 (2017) 254-264.
[60] C. Cao, S.N. Vasilatos, R. Bhargava, J.L. Fine, S. Oesterreich, N.E. Davidson, Y. Huang, Functional interaction of histone deacetylase 5 (HDAC5) and lysine-specific demethylase 1 (LSD1) promotes breast cancer progression, Oncogene, 36 (2017) 133-145.
[61] P.H. Huang, C.H. Chen, C.C. Chou, A.M. Sargeant, S.K. Kulp, C.M. Teng, J.C. Byrd, C.S. Chen, Histone deacetylase inhibitors stimulate histone H3 lysine 4 methylation in part via transcriptional repression of histone H3 lysine 4 demethylases, Mol Pharmacol, 79 (2011) 197-206.
[62] M.G. Lee, C. Wynder, D.A. Bochar, M.A. Hakimi, N. Cooch, R. Shiekhattar, Functional interplay between histone demethylase and deacetylase enzymes, Mol Cell Biol, 26 (2006) 6395-6402.
[63] M.M. Singh, C.A. Manton, K.P. Bhat, W.W. Tsai, K. Aldape, M.C. Barton, J. Chandra, Inhibition of LSD1 sensitizes glioblastoma cells to histone deacetylase inhibitors, Neuro Oncol, 13 (2011) 894-903.
[64] Y. Huang, S.N. Vasilatos, L. Boric, P.G. Shaw, N.E. Davidson, Inhibitors of histone demethylation and histone deacetylation cooperate in regulating gene expression and inhibiting growth in human breast cancer cells, Breast Cancer Res Treat, 131 (2012) 777-789.
[65] S.N. Vasilatos, T.A. Katz, S. Oesterreich, Y. Wan, N.E. Davidson, Y. Huang, Crosstalk between lysine-specific demethylase 1 (LSD1) and histone deacetylases mediates antineoplastic efficacy of HDAC inhibitors in human breast cancer cells, Carcinogenesis, 34 (2013) 1196-1207.
[66] S.S. W Fiskus, B Shah, BP Portier, SGT Devaraj1, K Liu, SP Iyer, D Bearss and KN Bhalla, Highly effective combination of LSD1 (KDM1A) antagonis and pan-histone deacetylase inhibitor against human AML cells, Leukemia, 28 (2014) 2155-2164.
[67] M.M. Singh, B. Johnson, A. Venkatarayan, E.R. Flores, J. Zhang, X. Su, M. Barton, F. Lang, J. Chandra, Preclinical activity of combined HDAC and KDM1A inhibition in glioblastoma, Neuro Oncol, 17 (2015) 1463-1473.
[68] H.P. Mohammad, K.N. Smitheman, C.D. Kamat, D. Soong, K.E. Federowicz, G.S. Van Aller, J.L. Schneck, J.D. Carson, Y. Liu, M. Butticello, W.G. Bonnette, S.A. Gorman, Y. Degenhardt, Y. Bai, M.T. McCabe, M.B. Pappalardi, J. Kasparec, X. Tian, K.C. McNulty, M. Rouse, P. McDevitt, T. Ho, M. Crouthamel, T.K. Hart, N.O. Concha, C.F. McHugh, W.H. Miller, D. Dhanak, P.J. Tummino, C.L. Carpenter, N.W. Johnson, C.L. Hann, R.G. Kruger, A DNA Hypomethylation Signature Predicts Antitumor Activity of LSD1 Inhibitors in SCLC, Cancer Cell, 28 (2015) 57-69.

[69] D.M.Z.S.a.D.G. McCafferty, trans-2-Phenylcyclopropylamine Is a Mechanism-Based Inactivator of the Histone Demethylase LSD1, Biochemistry 46 (2007) 4408-4416.
[70] B.E. Lauffer, R. Mintzer, R. Fong, S. Mukund, C. Tam, I. Zilberleyb, B. Flicke, A. Ritscher, G. Fedorowicz, R. Vallero, D.F. Ortwine, J. Gunzner, Z. Modrusan, L. Neumann, C.M. Koth, P.J. Lupardus, J.S. Kaminker, C.E. Heise, P. Steiner, Histone deacetylase (HDAC) inhibitor kinetic rate constants correlate with cellular histone acetylation but not transcription and cell viability, J Biol Chem, 288 (2013) 26926-26943.

Fig. 1. Reported representative LSD1 inhibitors.

Fig. 2. FDA approved HDAC inhibitors.

Fig. 3. Effect of histone methylation (A) and histone acetylation (B) in MGC-803 cells after 24 h treatment with compound **7** at 1.0 and 2.0 μM or SAHA at 2.0 μM using western blot analysis.

Fig. 4. Quantitative analysis of apoptotic cells using PI/AnnexinV-FITC double staining and flow-cytometry calculation. (A) MGC-803 cells were treated with compound **7** (0, 2.5, 5.0, 7.5 μM) for 24 h; (B) MGC-803 cells were treated with compound 7 (0, 2.5, 5.0, 7.5 μM) for 48 h.

Fig. 5. Changes of mitochondrial membrane potential after MGC-803 cells were treated with different concentrations of compound **7** (0, 2.5, 5.0 and 7.5μM) for 48 h.

Fig. 6. Binding models of tranylcypromine derivates with LSD1. (A) The co-crystal structure of the complex with GSK2699537 (yellow), FAD (green), and LSD1/CoREST. The residues are shown in cyan lines, H-bonds are shown in black dash line. (B) Predicted binding model of compound **7** with LSD1. Compound **7** and FAD are shown in cyan and green sticks, respectively; the residues are shown in brick lines, H-bonds are shown in green dash line, and the distance of FAD and compound **7** is shown in magenta.

Fig. 7. Predicted binding mode of compound **7** with HDAC2 (PDB: 4LXZ). (A) Interactions between compound 1 and HDAC2 residues. Compound **7** is shown as cyan sticks and residues are shown as brick lines. Zn^{2+} is shown as purple sphere. Hydrogen bonds are shown as green lines. (B) The surface on the rim of the binding site of compound **7** with HDAC2. Green area represents hydrophobic regions and red area represents exposed region.

Table 1 *In vitro* Inhibition of LSD1, MAO-A and MAO-B

Table 2 *In vitro* inhibitory activities of target compounds against HDAC isozymes

Table 3 *In vitro* antiproliferative activity of target compounds in five cancer cell lines

Table 4 Calculated physicochemical and ADME parameters the tested compounds

Scheme 1. Synthesis of compounds **1**-7. Reagents and conditions: (a) $(Boc)_2O$, Et_3N, CH_2Cl_2, 0^oC-rt, 4h; (b) NaH, methyl 4-(bromomethyl)benzoate, dry DMF, 0^oC-rt, 0.5 h; (c) LiOH, THF-H_2O (1:1), rt, overnight; (d) HBTU, Et_3N, 0^oC-rt, 2-6 h; (e) NH_2OH, KOH, dry CH_3OH, 0^oC-rt, 3 h; (f) CF_3COOH, dry CH_2Cl_2, 0^oC-rt, 3-8 h.

Scheme 2. Synthesis of compounds **8-11**. Reagents and conditions: (a) NaH, methyl 3-(4-Bromomethyl)cinnamate, dry DMF, 0^oC-rt, 0.5 h; (b) LiOH, THF-H_2O (1:1), rt, overnight; (c) HBTU, Et_3N, 0^oC-rt, 2-4 h; (d) CF_3COOH, dry CH_2Cl_2, 0^oC-rt, 3-8 h.

Table 1 *In Vitro* Inhibition of LSD1, MAO-A and MAO-B

Compounds	IC_{50} (μM)[a]		
	LSD1	MAO-A	MAO-B
5a	4.09±0.36	45.84±3.17	> 100
5b	7.16±0.54	50.07±3.06	> 100
7	1.20±0.09	21.11±2.03	87.09±2.96
11a	2.21±0.33	39.41±1.75	> 100
11b	3.85±0.73	36.89±2.27	> 100
SAHA	> 100	> 100	> 100
2-PCPA	29.31±2.35	4.72±1.04	2.95±0.81
Clorgyline	ND[b]	0.0036[c]	ND
R(-)-deprenyl	ND	ND	0.094[c]

[a] Data are represented as IC_{50} values (mean ± SD). All experiments were independently carried out at least three times.
[b] ND: no detection
[c] Values are the mean of two experiments.

Table 2 *In vitro* inhibitory activities of target compounds against HDAC isozymes

Compounds	IC_{50} (nM)[a]		
	HDAC1	HDAC2	HDAC5
5a	1436	3103	NI[b]
5b	218	413	NI
7	15	23	16840
11a	12	25	2967
11b	314	491	NI
SAHA	16	28	ND[c]
TMP269	ND	ND	990

[a] Values are the mean of two experiments.
[b] NI: no inhibition
[c] ND: no detection

Table 3 *In vitro* antiproliferative activity of target compounds in five cancer cell lines

Compounds	IC_{50} (μM)[a]				
	MGC-803	MCF-7	SW-620	PC-3	A-549
5a	12.04±1.19	17.27±2.06	23.27±2.14	19.76±1.03	6.75±0.35
5b	21.47±2.88	19.48±1.39	>32	21.69±2.31	5.36±0.46
7	0.81±0.07	4.28±1.10	2.35±0.13	5.48±0.54	1.34±0.12
11a	2.46±0.32	6.24±1.21	4.03±0.88	5.62±0.67	1.41±0.18
11b	13.56±1.30	22.09±2.36	26.86±3.08	11.60±1.91	3.17±0.19
SAHA	8.75±0.93	4.69±1.36	3.87±0.74	3.46±0.85	2.39±0.43

[a] IC_{50} values are expressed as mean ± SD from at least three independent experiments.

Table 4 Calculated physicochemical and ADMET parameters of the target compounds

Comp	Lipinski's Parameters					TPSA[f]	CYP-3A4[g]	CYP-2C19[h]	Carcino-rat[i]
	LogP[a]	MW[b]	nON[c]	nOHNH[d]	nviolations[e]				
5a	2.1	282.3	4	3	0	61.4	Non	Non	negative
5b	3.5	357.5	4	4	0	67.2	Non	Non	negative
7	3.2	409.5	6	4	0	90.5	Non	Non	negative
11a	2.7	308.4	4	3	0	61.4	Non	Non	negative
11b	4.2	383.5	4	4	0	67.2	Non	Non	negative

[a] Calculated lipophilicity.
[b] Molecular weight.
[c] Number of hydrogen bond acceptor.
[d] Number of hydrogen bond donor.
[e] Number of violation from Lipinski's rule of five.
[f] Total polar surface area.
[g] In vitro Cytochrome P450 3A4 inhibition.
[h] In vitro Cytochrome P450 2C19 inhibition.
[i] 2 years carcinogenicity bioassay in rat.

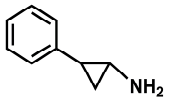

2-PCPA

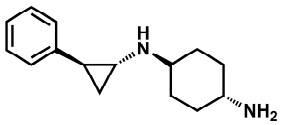

1, ORY-1001

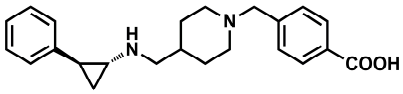

2, GSK2879552

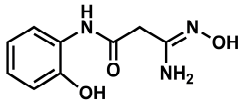

3

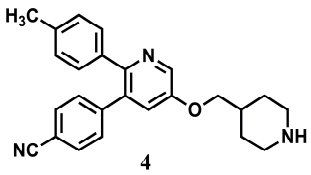

4

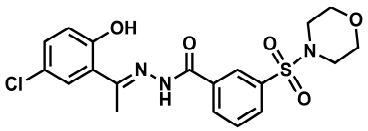

5

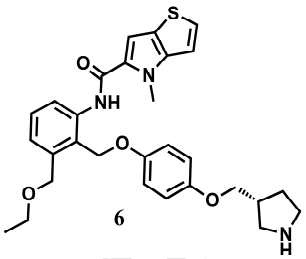

6

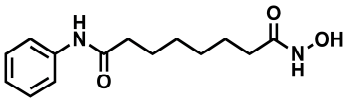

SAHA(Vorinostat)

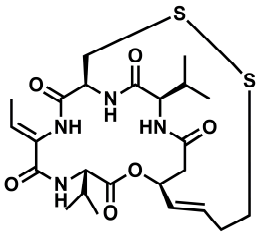

Romidepsine

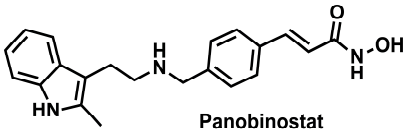

Panobinostat

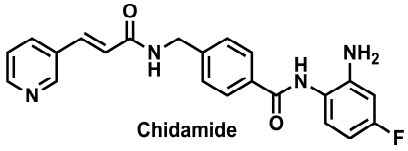

Chidamide

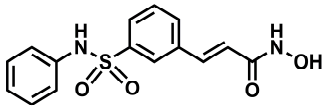

Belinostat

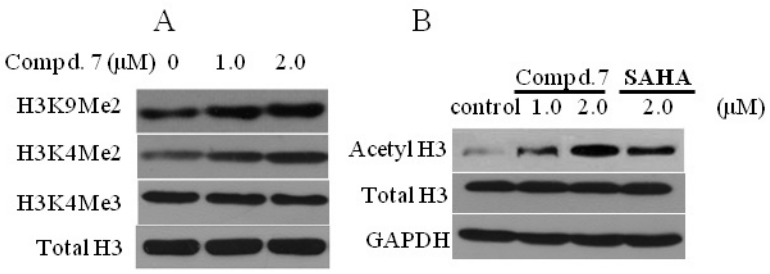

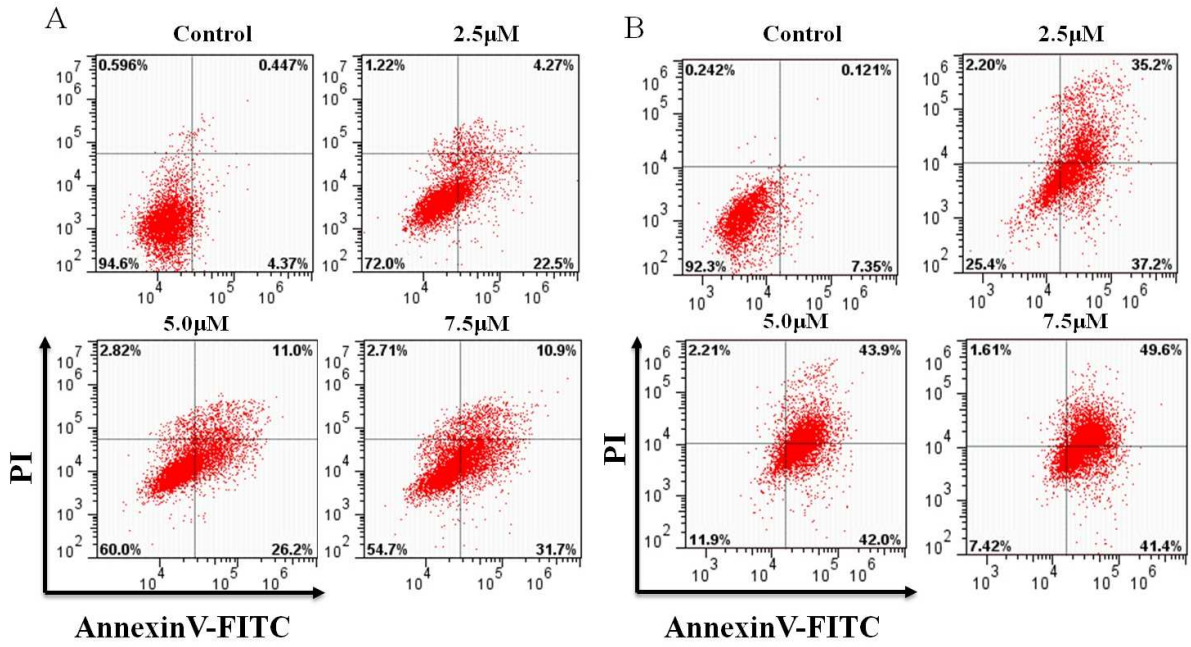

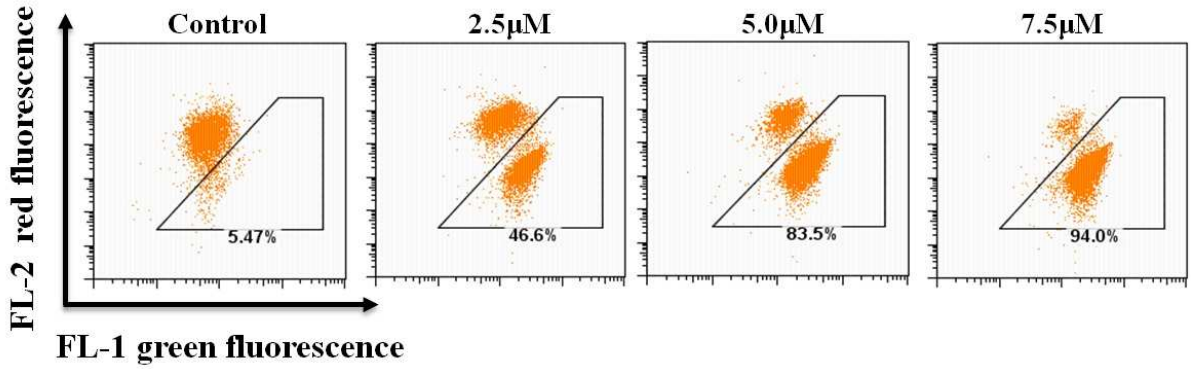

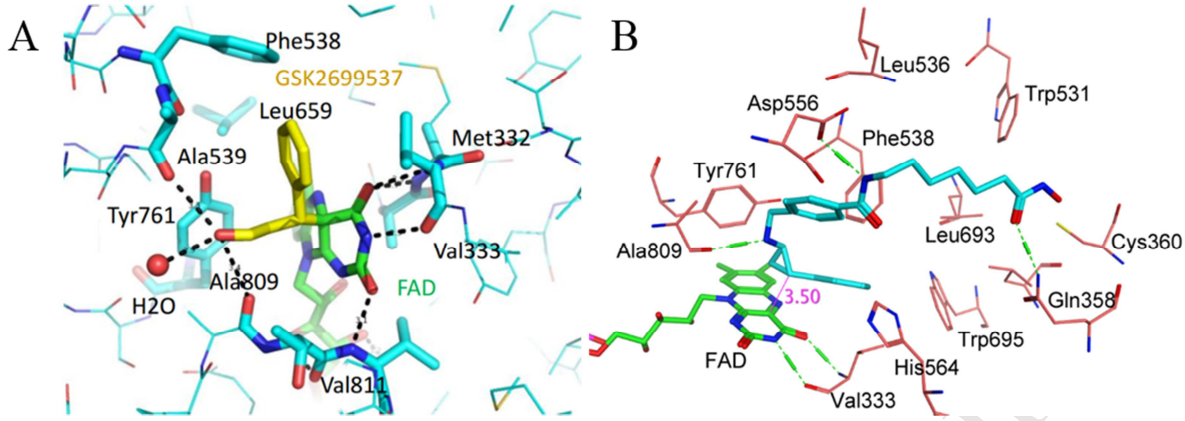

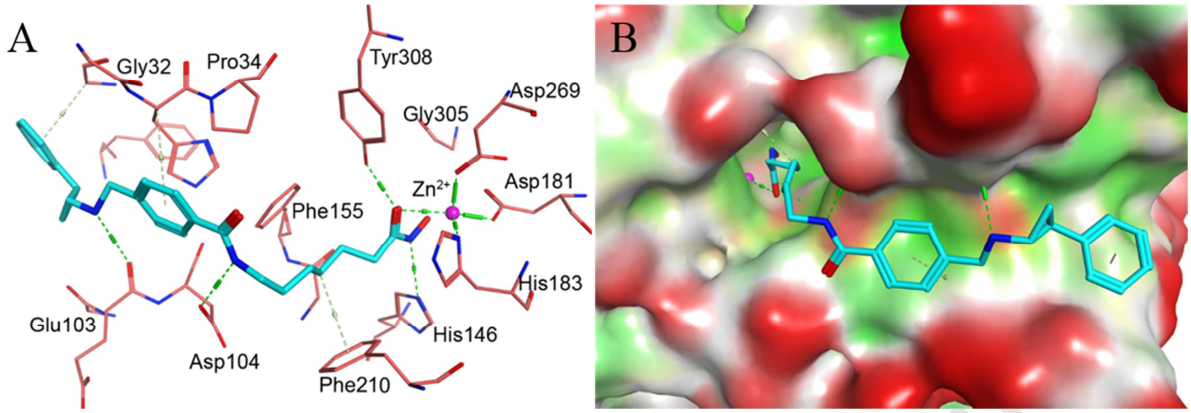

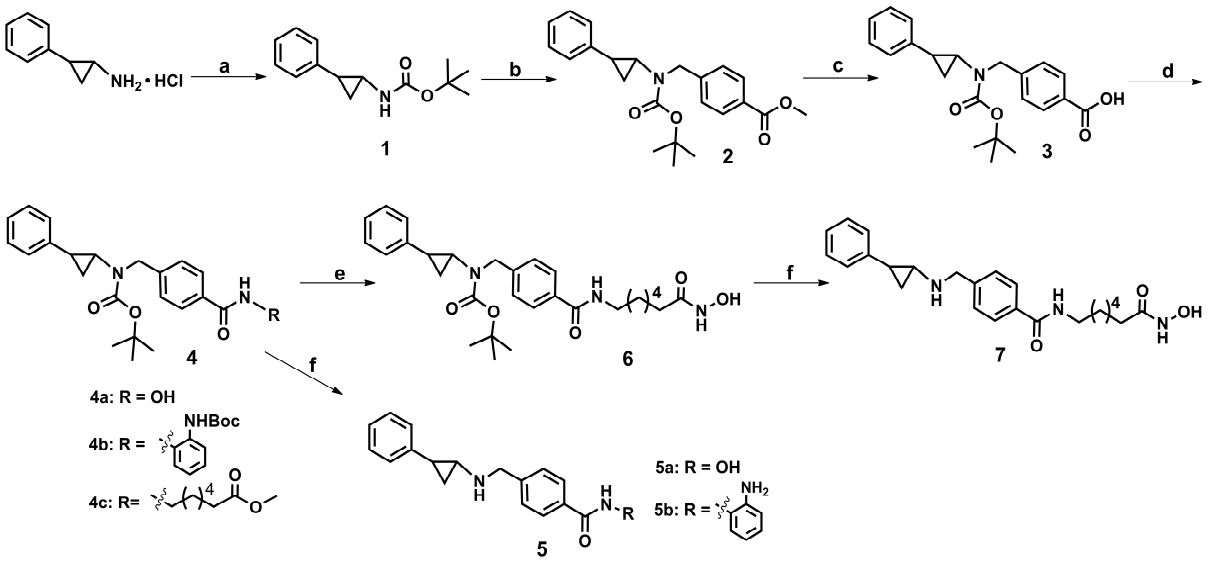

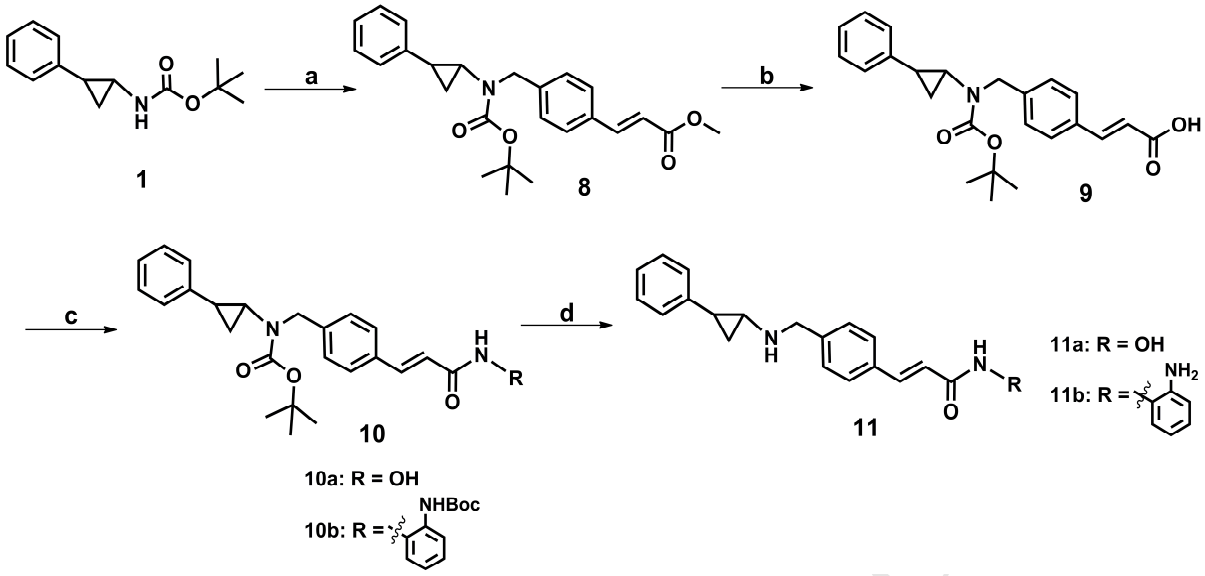

Highlights

- A series of tranylcypromine derivatives were discovered as novel LSD1/HDACs dual inhibitors.
- Compound **7** exhibited potent dual LSD1/HDACs inhibition with strong antiproliferative activity.
- Compound **7** dose-dependently increased cellular H3K4 and H3K9 methylation, as well as H3 acetylation.
- Compounds **7** induced remarkable apoptosis and decreased mitochondrial membrane potential.